Journal of Applied Polymer Science

Design and synthesis of organosoluble and transparent polyimides containing bulky substituents and noncoplanar structures

Xiaohua Huang,[1] Xianglin Pei,[1] Lichun Wang,[2] Mei Mei,[1] Chanjuan Liu,[1,3] Chun Wei[1]

[1]Key Laboratory of New Processing Technology for Nonferrous Metal and Materials (Ministry of Education), School of Material Science and Engineering, Guilin University of Technology, Guilin 541004, People's Republic of China

[2]NanTong Polymax Elastomer Technology Company, Limited, Nantong 226011, China

[3]Ministry of Education Key Laboratory for the Chemistry and Molecular Engineering of Medicinal Resources, School of Chemistry and Pharmaceutical Science, Guangxi Normal University, Guilin 541004, People's Republic of China

Correspondence to: X. Huang (E-mail: huangxiaohua@glut.edu.cn) and C. Liu (E-mail: liuchanjuan@glut.edu.cn)

ABSTRACT: A new diamine monomer, 3,3′-diisopropyl-4,4′-diaminophenyl-4″-phenyltouene, was designed, synthesized, and then polymerized with five commercial dianhydrides to obtain a series of novel polyimides via a one-step method. The obtained polymers showed excellent solubility in most common solvents, even in low-boiling solvents, such as chloroform, dichloromethane, and tetrahydrofuran. They exhibited a high thermal stability with the glass-transition temperature in the range 262–318°C and 10% weight loss temperatures in the range 464–488°C under a nitrogen atmospheres. Meanwhile, these polymer films also displayed a high optical transparency with a cutoff wavelength in the range 305–365 nm; prominent mechanical properties with a tensile strength of 65.6–94.9 MPa, a Young's modulus of 1.6–2.8 GPa, and an elongation at break of 9.3–13.7%; a low dielectric constant in the range of 2.91–3.18 at 1 MHz; and an outstanding hydrophobicity with a contact angle above 90.6°. © 2015 Wiley Periodicals, Inc. J. Appl. Polym. Sci. **2016**, *133*, 43266.

KEYWORDS: films; optical properties; polyimides; thermal properties

Received 23 September 2015; accepted 23 November 2015
DOI: 10.1002/app.43266

INTRODUCTION

As outstanding high-performance polymer materials, aromatic polyimides (PIs) have been studied extensively because of their prominent thermal stability, good chemical resistance, and excellent mechanical and electrical properties. So far, PIs have been widely used in many applications, such as microelectronics, optoelectronics, passivation coatings, and integrated electronic circuits.[1–3] However, wholly aromatic PIs still exhibit some drawbacks; for example, they are usually insoluble and infusible because of the rigidity of their backbones[4] and low optical transparency properties with a deep color.[5] This further limits their applications.

Many efforts to chemically modify PIs have been made to overcome these weaknesses; these efforts include the introduction of bulky units or bulky pendent substituents[6–11] and the twisting of noncoplanar structures,[12–16] unsymmetrical structures,[17–21] and flexible linkages[22–25] into the polymer backbones. However, the glass-transition temperature (T_g) values of polymers containing flexible units will be greatly decreased because of the abundant flexible linkages in the macromolecular backbones.[26] Recently, considerable attention has been devoted to the study of fluorinated PIs.[27,28] Fluorination improves solubility and optical, hydrophobic, and dielectric performances of PIs because of the incorporation of fluorinated groups. However, the cost of fluorochemicals is usually very high, and this limits further application. Therefore, to overcome these drawbacks, as stated previously, the reduction of the cost of the monomer and the maintenance of excellent comprehensive properties of polymers without the sacrifice of their thermal and mechanical properties are the main design direction for chemical modifications.[29,30] Huang *et al.*[31] reported some novel PIs; the polymers presented excellent solubility in most organic solvents and displayed good thermal stability and optical properties. Liaw *et al.*[32] prepared several novel poly(pyridine imide)s with pendent naphthalene groups; these PIs showed excellent solubility and good thermal properties.

Compared with the previous research, in this study, we attempted to provide a new approach for the design and synthesis of one kind of high-performance polymer material with excellent organosolubility and transparency without compromise of its thermal stability and mechanical properties. In this

study, a series of novel PIs containing bulky isopropyl and biphenyl moieties and a large twist of noncoplanar structures were prepared from a rigid aromatic diamine monomer, 3,3′-diisopropyl-4,4′-diaminophenyl-4″-phenyltouene (PAPT), with the synergism of bulky substituents and noncoplanar structures to obtain a series of organosoluble and transparent PIs. Moreover, the optical properties, hydrophobic properties, mechanical properties, and dielectric constants of the polymers were investigated.

EXPERIMENTAL

Materials

4-Biphenyl carboxaldehyde (TCI Chemical Co., Ltd.) and 2-isopropyl aniline (Aldrich Chemical Co., Ltd.) were used as received. Commercial pyromellitic dianhydride (PMDA; Shanghai Guoyao Chemical Co., Ltd.), biphenyl tetracarboxylic dianhydride (BPDA), oxydiphthalic anhydride (ODPA; Changzhou Linchuan Chemical Co., Ltd.), benzophenone tetracarboxylic dianhydride (BTDA), and 4,4′-(hexafluoroisopropylidene)-diphthalic anhydride (6FDA; Tokyo Chemical Industry Co., Ltd.) were recrystallized in acetic anhydride and then dried in vacuums at 120°C for 12 h before use. Solvents, such as *N,N*-dimethylformamide (DMF) and *m*-cresol (Shanghai Guoyao Chemical Co., Ltd.) were purified by distillation over calcium hydride under reduced pressure. All of the other reagents, including *N,N*-dimethylacetamide (DMAc), *N*-methyl-2-pyrrolidone (NMP), dichloromethane (CH_2Cl_2), and chloroform ($CHCl_3$), were purchased from various merchants and were used without further purification.

Measurements

Fourier transform infrared (FTIR) spectra were taken with a Thermo Nexus 470 FTIR spectrometer. Mass spectrometry (MS) was measured on an Elementar Vario EL III/Isoprime. Elemental analysis was performed with a PerkinElmer model 2400 II system. NMR spectra were obtained with a 400-MHz Bruker instrument with hexadeuterated dimethyl sulfoxide (DMSO-d_6) or $CDCl_3$ as the solvent. Gel permeation chromatography (GPC) was performed on a Waters 1515 analyzer relative to a polystyrene standard with DMF as the eluent. Differential scanning calorimetry (DSC) was run on a Netzsch 204 DSC instrument at a heating rate of 10°C/min under a nitrogen atmosphere. Thermogravimetric analysis (TGA) was conducted on a TGA Q500 analyzer at a heating rate of 10°C/min under a nitrogen atmosphere. Ultraviolet–visible (UV–vis) spectroscopy was done on a 3600 UV–vis spectrophotometer at room temperature. The contact angle of the polymer film for water was recorded on a JY-PHb contact angle analysis system. The mechanical properties of the films were measured with a AG-I 50 KN, and the size of each film was about 50 × 5 × 0.05 mm^3.

Monomer Synthesis: PAPT

A mixture of 4-biphenyl carboxaldehyde (15.00 g, 0.082 mol) and 2-isopropyl aniline (27.83 g, 0.21 mol) was placed in a 250-mL, three-necked flask equipped with a magnetic stirrer, a condenser, and a dropping funnel, and then, 3.7 mL of hydrochloric acid (HCl; 12*N*) was added dropwise over 1 h at 80°C under a nitrogen atmosphere. After the addition, the reaction mixture was heated to reflux at 150°C for another 10 h. After the reaction was completed, the resulting suspension was cooled to about 60°C, neutralized with a 10% aqueous solution of sodium hydroxide (25.0 mL), extracted with CH_2Cl_2, and washed with deionized water several times. The mixture solution was dried overnight by anhydrous magnesium sulfate, filtered, and evaporated to obtain a white solid powder. After that, the crude product was recrystallized from ethanol to obtain pure white crystals (PAPT).

Yield = 68%, mp = 157°C. ^{1}H-NMR (δ, ppm, DMSO-d_6): 7.61 (d, 2H, J = 5.2 Hz), 7.54 (d, 2H, J = 6.4 Hz), 7.41 (t, 2H, J = 7.6), 7.30 (t, 1H, J = 8 Hz), 7.13 (d, 2H, J = 7.2 Hz), 6.81 (s, 2H), 6.60 (d, 2H, J = 8.8 Hz), 6.51 (d, 2H, J = 6.8 Hz), 5.21 (s, H), 4.69 (s, 4H), 2.88–2.94 (m, 2H, J = 6 Hz), 1.04 (d, 12H, J = 4 Hz). ^{13}C-NMR (δ, ppm, DMSO-d_6): 146.19, 143.86, 140.66, 137.94, 132.94, 131.47, 130.04, 129.54, 127.81, 127.26, 127.13, 126.97, 126.08, 115.25, 55.54, 27.08, 23.11. FTIR spectroscopy (KBr, cm^{-1}): 3500–3200 (—NH_2, br, s), 2960–2870 (C—H, br, s). MS (mass-to-charge ratio): 435.28 ($[M+H]^+$).

Polymer Synthesis

All of the PIs were prepared by a conventional one-step procedure. The synthesis of PI-3 (PAPT–ODPA) derived from PAPT and ODPA as a typical example was done as follows. Into a 50-mL, three-necked flask equipped with a mechanical stirrer, a condenser, and an inlet and outlet of nitrogen were placed PAPT (0.9941 g, 2.29 mmol), ODPA (0.7096 g, 2.29 mmol), 15.3 mL of *m*-Cresol, and five drops of isoquinoline. The mixture was stirred at room temperature for 30 min and then heated to 50°C until a brown transparent solution was formed. Then, the mixture was stirred further for 10 h at 120°C, 4 h at 180°C, and 22 h at 200°C. After the reaction, the polymer solution was slowly poured into 500 mL of ethanol to get a fibrous precipitate, filtered, and dried *in vacuo* at 150°C for 12 h to obtain the polymer PI-3. The PI-1 (PAPT–PMDA), PI-2 (PAPT–BPDA), PI-4 (PAPT–BTDA), and PI-5 (PAPT–6FDA) were also obtained by a method similar to that discussed previously.

PI-1. Yield = 93%. FTIR spectroscopy (KBr, cm^{-1}): 3029–2870 (alkyl, br, s), 1778 and 1725 (C═O, imide, stretching vibrations, vs), 1372 (C—N, s), 729 (C═O, imide, bending vibrations, vs). ^{1}H-NMR (400 MHz, $CDCl_3$, ppm): 8.52 (s, 2H, ArH), 7.59–7.64 (m, 4H, ArH), 7.45 (t, 2H, J = 7.8 Hz, ArH), 7.28–7.37 (m, 5H, ArH), 7.12–7.16 (m, 4H, ArH), 5.71 (s, 1H, CH), 2.69–2.78 [m, 2H, $CH(CH_3)_2$], 1.15 (d, 12H, J = 4.8 Hz, CH_3). ANAL. Calcd for $(C_{41}H_{32}N_2O_4)_n$: C, 79.85%, N, 4.54%. Found: C, 79.04%, N, 4.62%.

PI-2. Yield = 94%. FTIR spectroscopy (KBr, cm^{-1}): 3028–2869 (alkyl, br, s), 1777 and 1730 (C═O, imide, stretching vibrations, vs), 1372 (C—N, s), 742 (C═O, imide, bending vibrations, vs). ^{1}H-NMR (400 MHz, $CDCl_3$, ppm): 8.26 (s, 2H, ArH), 8.08–8.13 (m, 4H, ArH), 7.66–7.59 (m, 4H, ArH), 7.45 (t, 2H, J = 7.6 Hz, ArH), 7.28–7.37 (m, 5H, ArH), 7.11–7.16 (m, 4H, ArH), 5.70 (s, 1H, CH), 2.79–2.85 [m, 2H, $CH(CH_3)_2$], 1.16 (d, 12H, J = 6.4 Hz, CH_3). ANAL. Calcd for $(C_{47}H_{36}N_2O_4)_n$: C, 81.48%, N, 4.04%. Found: C, 82.11%, N, 3.92%.

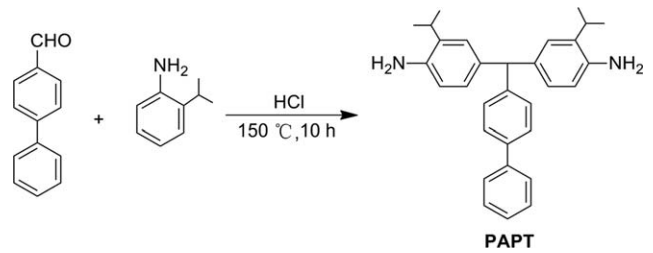

Scheme 1. Synthesis of the diamine monomer PAPT.

PI-3. Yield = 92%. FTIR spectroscopy (KBr, cm^{-1}): 3029–2869 (alkyl, br, s), 1778 and 1727 (C═O, imide, stretching vibrations, vs), 1375 (C—N, s), 748 (C═O, imide, bending vibrations, vs). ^{1}H-NMR (400 MHz, $CDCl_3$, ppm): 8.01 (d, 2H, J = 8.0 Hz, ArH), 7.56–7.64 (m, 6H, ArH), 7.51 (d, 2H, J = 8.4 Hz, ArH), 7.44 (t, 2H, J = 7.6 Hz, ArH), 7.27–7.36 (m, 5H, ArH), 7.09–7.14 (m, 4H, ArH), 5.68 (s, 1H, CH), 2.77–2.85 [m, 2H, $CH(CH_3)_2$], 1.15 (d, 12H, J = 6.4 Hz, CH_3). Anal. Calcd for $(C_{47}H_{36}N_2O_5)_n$: C, 79.64%, N, 3.95%. Found: C, 80.27%, N, 3.79%.

PI-4. Yield = 95%. FTIR spectroscopy (KBr, cm^{-1}): 3028–2870 (alkyl, br, s), 1779 and 1731 (C═O, imide, stretching vibrations, vs), 1378 (C—N, s), 725 (C═O, imide, bending vibrations, vs). ^{1}H-NMR (400 MHz, $CDCl_3$, ppm): 8.28–8.32 (m, 4H, ArH), 8.16 (d, 2H, J = 18.8 Hz, ArH), 7.57–7.63 (m, 4H, ArH), 7.44 (t, 2H, J = 7.6 Hz, ArH), 7.27–7.36 (m, 5H, ArH), 7.07–7.17 (m, 4H, ArH), 5.70 (s, 1H, CH), 2.84–2.76 [m, 2H, $CH(CH_3)_2$], 1.15 (d, 12H, J = 6.8 Hz,CH_3). Anal. Calcd for $(C_{48}H_{36}N_2O_5)_n$: C, 79.98%, N, 3.89%. Found: C, 79.43%, N, 4.01%.

PI-5. Yield = 93%. FTIR spectroscopy (KBr, cm^{-1}): 3030–2871 (alkyl, br, s), 1786 and 1731 (C═O, imide, stretching vibrations, vs), 1375 (C—N, s), 723 (C═O, imide, bending vibrations, vs). ^{1}H-NMR (400 MHz, $CDCl_3$, ppm): 8.05 (d, 2H, J = 2.8 Hz, ArH), 7.91–7.95 (m, 4H, ArH), 7.58–7.63 (m, 4H, ArH), 7.44 (t, 2H, J = 7.6 Hz, ArH), 7.27–7.36 (m, 5H, ArH), 7.08–7.14 (m, 4H, ArH), 5.68 (s, 1H, CH), 2.78–2.82 [m, 2H, $CH(CH_3)_2$], 1.15 (d, 12H, J = 6.0 Hz, CH_3). Anal. Calcd for $(C_{50}H_{36}F_6N_2O_4)_n$: C, 71.25%, N, 3.32%. Found: C, 72.44%, N, 3.21%.

Preparation of the PI Films

The PI films were prepared by solution casting. For example, 0.4 g of polymer was dissolved into about 4.0 mL of DMF and then poured onto a 6 × 6 cm^2 clean glass plate and placed in an oven at 60°C for 24 h until most of the DMF was evaporated. After they were cooled to room temperature, the films were immersed in deionized water to strip the samples from the glass plates and dried in a vacuum oven at 180°C for another 12 h to obtain PI films with a thickness of about 50 μm. In the same way, 0.015 g of polymer, 1.0 mL of DMF, and a 3 × 3 cm^2 glass plate were used to obtain PI films with a thickness of about 10–15 μm under the same conditions.

RESULTS AND DISCUSSION

Monomer Synthesis

The synthetic route of aromatic diamine PAPT is shown in Scheme 1. The structure of PAPT was characterized by FTIR spectroscopy, NMR, elemental analysis, and MS. The FTIR spectra showed the characteristic absorption bands of the amino groups (N—H) at 3500–3200 cm^{-1} and the alkyl groups (C—H) at 2960–2870 cm^{-1}. The structure of the diamine monomer was also confirmed by ^{1}H-NMR and ^{13}C-NMR spectra, and the typical spectra are shown in Figure 1. The ^{1}H-NMR spectrum of PAPT showed the characteristic aromatic C—H peaks appearing at 7.61–6.51 ppm, the characteristic resonance signals (^{i}H) of the amine (—NH_2) were observed at 4.69 ppm, and the signals at 5.21, 2.92, and 1.04 ppm were ascribed to the protons of the alkyl —CH— (^{i}H), —CH— (^{k}H), and —CH_3 (^{l}H) groups, respectively. The ^{13}C-NMR spectrum exhibited 17 carbon peaks in accordance with the structure of the designed compound. Moreover, the MS data and elemental analysis values were in good agreement with the proposed structures.

Polymer Synthesis

The general one-step procedure for the preparation of the polymers is illustrated in Scheme 2. The obtained diamine monomer, PAPT, was reacted with five commercial dianhydrides, respectively, to obtain a series of novel PIs by a one-step, high-temperature polycondensation. The structures of the resulting polymers were identified by FTIR spectroscopy, ^{1}H-NMR, elemental analysis, and GPC. The testing data of elemental analysis and GPC are listed in Table I. The results of GPC showed that the weight-average molecular weight (M_w) and polydispersity

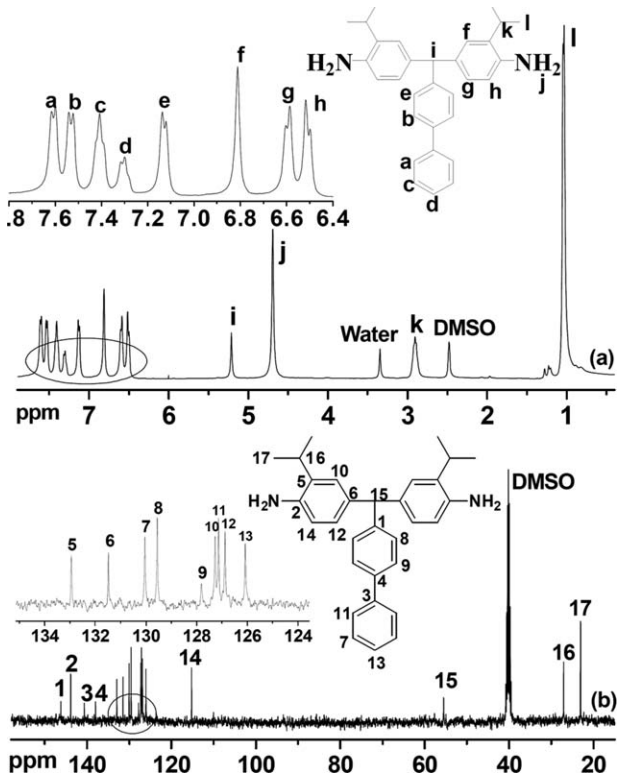

Figure 1. (a) ^{1}H-NMR and (b) ^{13}C-NMR spectra of diamine.

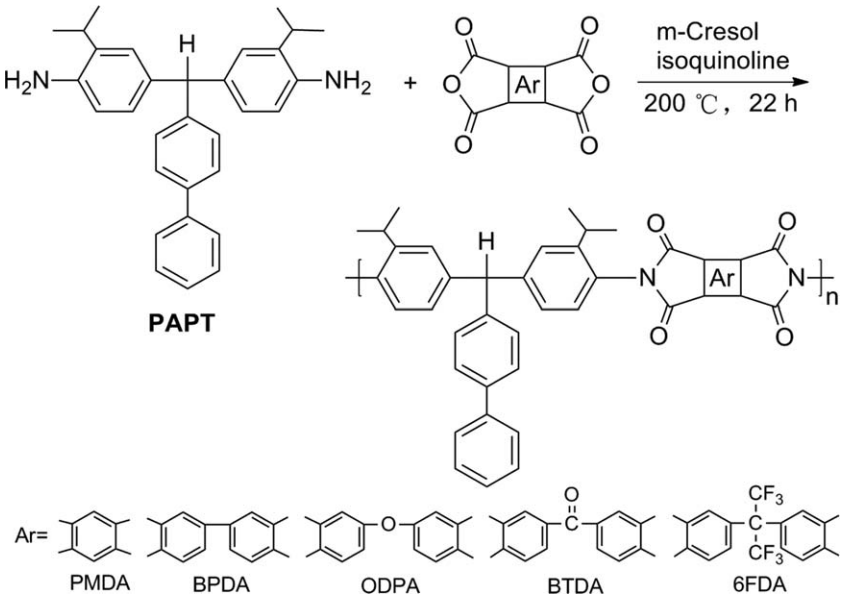

Scheme 2. Synthesis of the PIs.

index [M_w/number-average molecular weight (M_n)] values were in the range 0.9 × 10^5 to 5.8 × 10^5 g/mol and 1.6–2.3, respectively, and these PIs presented high-molecular-weight and low-molecular-weight distributions. Obviously, PI-2 presented the highest molecular weight; its value was far higher than those of the other polymers, and this may have been because of the results of the partial crosslinking reaction during polymerization. Meanwhile, the elemental analysis was in good accordance with the calculated results; this also further illustrated the structure of the polymers. Figure 2 outlines the FTIR spectra of the polymers, and the disappearance of the absorption bands at 3500–3200 cm^{-1} completely proved the imidization of the polymerization. The peaks at 3030–2870 cm^{-1} were assigned to alkyl groups. The peaks around at 1777, 1727, and 729 cm^{-1} were attributed to the characteristic imide absorption bands, and the peaks at 1375 cm^{-1} were ascribed to the C—N stretching absorption peak. What is more, the structures of the PIs were also confirmed by ^{1}H-NMR and elemental analysis. The typical ^{1}H-NMR spectrum of PI-3 is shown in Figure 3. It presented broad peaks in the region 8.01–7.12 ppm for aromatic C—H bonds and peaks at 5.67, 2.81, and 1.15 ppm for the alkyls of ^{l}H, ^{m}H, and ^{n}H, respectively. In combination with the

Table I. GPC Data and Elemental Analyses of the PIs

	GPC data[a]			Elemental analysis (%)			
Polymer	$M_n \times 10^5$	$M_w \times 10^5$	M_w/M_n	Formula		C	N
PI-1	0.6	1.1	1.8	$(C_{41}H_{32}N_2O_4)_n$ $(616.70)_n$	Calculated	79.85	4.54
					Found	79.04	4.62
PI-2	2.9	5.8	2.0	$(C_{47}H_{36}N_2O_4)_n$ $(692.80)_n$	Calculated	81.48	4.04
					Found	82.11	3.92
PI-3	0.7	1.1	1.6	$(C_{47}H_{36}N_2O_5)_n$ $(708.80)_n$	Calculated	79.64	3.95
					Found	80.27	3.79
PI-4	0.4	0.9	2.3	$(C_{48}H_{36}N_2O_5)_n$ $(720.81)_n$	Calculated	79.98	3.89
					Found	79.43	4.01
PI-5	2.6	4.7	1.8	$(C_{50}H_{36}F_6N_2O_4)_n$ $(842.82)_n$	Calculated	71.25	3.32
					Found	72.44	3.21

[a] With respect to polystyrene standards with DMF as the eluent.

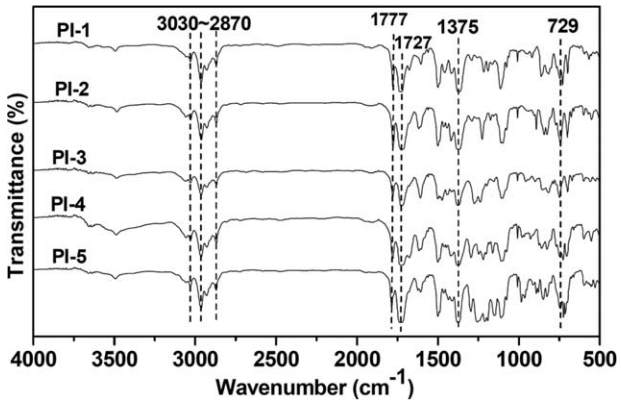

Figure 2. FTIR spectra of the PIs.

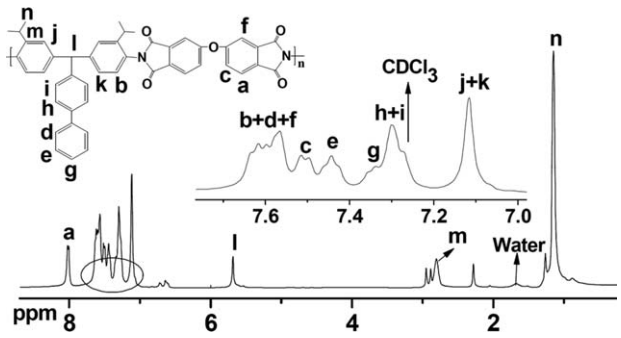

Figure 3. ^{1}H-NMR spectra of PI-3.

results of elemental analysis, this was also in complete agreement with the proposed polymer structures. Furthermore, as shown in Figure 4, the geometric structure of PAPT and its corresponding oligomer were simulated by CambridgeSoft Chem 3D. As shown in the red circle, the PAPT and corresponding oligomer presented a large twist of noncoplanar structure under an optimized energy state with the introduction of isopropyl and biphenyl moieties. Obviously, the incorporation of the nonplanar steric structure effectively decreased the strong interaction of intermolecular and intramolecular interactions and the tight stacking of the molecular chains. This may have rendered a kind of polymer with excellent organosolubility and transparency and without the sacrifice of their thermal stability and mechanical properties.[33]

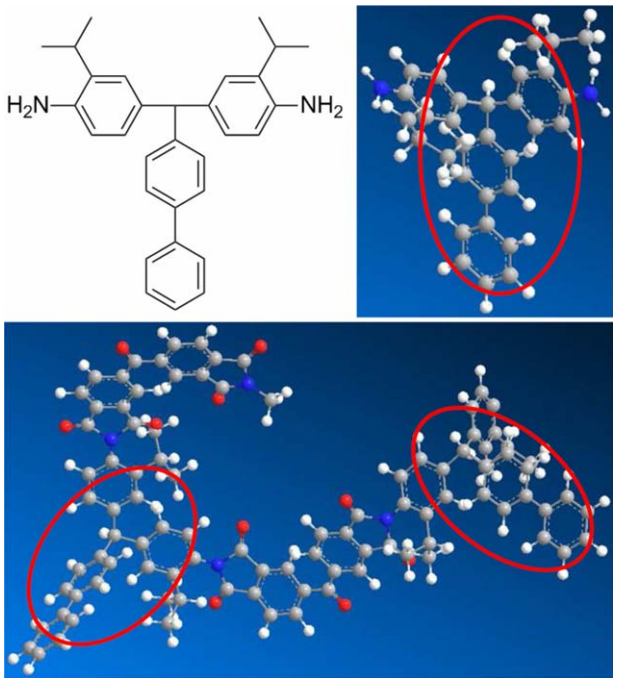

Figure 4. Three-dimensional structures of PAPT and its corresponding oligomer. [Color figure can be viewed in the online issue, which is available at wileyonlinelibrary.com.]

Polymer Solubility

The solubility of the polymers with a test concentration of 10 mg/mL is outlined in Table II. It was obvious that the obtained PIs could not only be soluble in high-boiling-point solvents, such as DMF, DMAc, dimethyl sulfoxide (DMSO), and NMP, but also in low-boiling-point solvents, such as $CHCl_3$, CH_2Cl_2, and tetrahydrofuran (THF). These PIs presented outstanding solubility properties, mainly because of the incorporation of the bulky isopropyl and biphenyl moieties in the polymer backbones, which formed noncoplanar structures and decreased the packing density, regularity, and intermolecular interactions in the polymer chains. Apparently, PI-2 prepared from BPDA partially dissolved in THF under the heating condition. This may have been due to the rigidity of the biphenyl structure and the higher molecular weight of the polymer. This decreased the solubility of PI-2. In acetone solvent testing, only PI-5 derived from 6FDA could dissolve rapidly at room

Table II. Solubility of the PIs

	Solvent									
Polymer	DMF	DMAc	DMSO	NMP	$CHCl_3$	CH_2Cl_2	THF	Acetone	EAC	*n*-Hexane
PI-1	++	++	++	++	++	++	++	−h	−−	−−
PI-2	++	++	++	++	++	++	−h	−h	−−	−−
PI-3	++	++	++	++	++	++	++	−h	−h	−−
PI-4	++	++	++	++	++	++	++	−h	−h	−−
PI-5	++	++	++	++	++	++	++	++	+h	−−

++, soluble at room temperature; +h, soluble under the heating condition; −h, partially soluble under the heating condition; −−, insoluble. The solubility was tested with a polymer concentration of 10 mg/mL in the solvent with stirring.

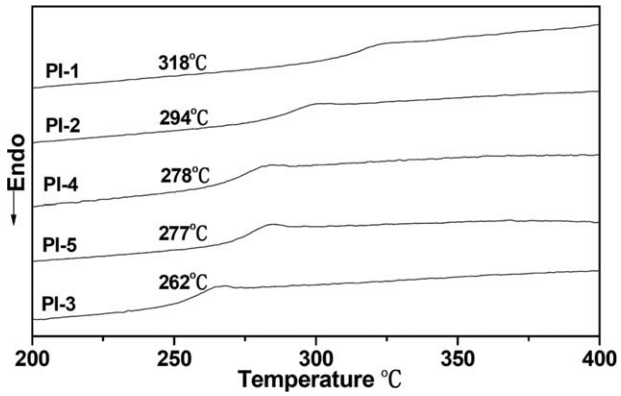

Figure 5. DSC curves of the PIs.

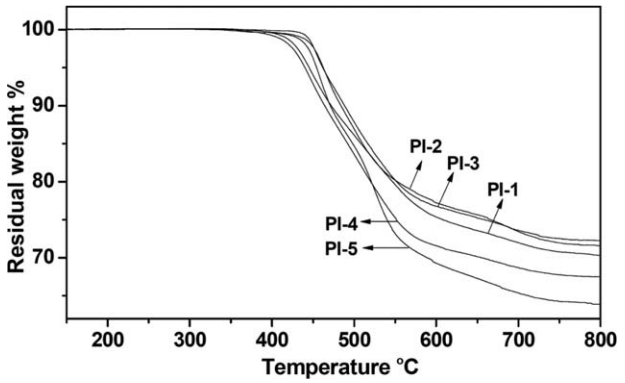

Figure 6. TGA curves of the PIs.

temperature. This was probably due to the incorporation of bulky —$(CF_3)_2$— groups in the main chain. This further reduced the packing density and interactions and intra-actions of the polymer chains. Obviously, PI-1 originating from PMDA and PI-2 originating from BPDA could not dissolve in ethyl acetate (EAC) because of the relative rigidity of pyromellitic and biphenyl units in the polymer chain. However, PI-3 originating from ODPA and PI-4 originating from BTDA were partially soluble in EAC under the heating condition because of the introduction of the relatively flexible ether and carbonyl groups in the polymer backbone. These polymers exhibited excellent solubility properties, and this gives them potential application in modern microelectronics, optoelectronics, flexible circuits, collapsible solar panels, and so on.[34–36]

Thermal Properties

Figure 5 shows the DSC curves of the PIs, and the test results are shown in Table III. All of the polymers showed high T_gs ranging from 262 to 318°C; these were mainly attributed to the introduction of the bulky substituent and the noncoplanar structure in the polymer chain, which then presented a higher rigidity. All of the obtained PIs were synthesized with the same diamine and different dianhydrides, and the differences in the T_g's among the polymers was mainly dependent on the structure of the aromatic dianhydride units in the polymer backbone. It was obvious that PI-1 based on PMDA showed the highest T_g (318°C), mainly because the polymer chain contained rigid pyromellitic units. PI-3 originating from ODPA presented a relatively low T_g value, mainly because of the flexibility of ether linkages in the polymer structure.

The thermal stability of the PIs was evaluated by TGA measurement under a nitrogen atmosphere. Figure 6 shows the TGA curves of the PIs, and the data are summarized in Table III. This indicated that these PIs presented excellent thermal stability. The values of the thermal onset decomposition temperature (T_d) were in the range 419–445°C, and the 5% and 10% weight loss temperatures ($T_{5\%}$ and $T_{10\%}$, respectively) were in the ranges 440–462 and 464–488°C, respectively. Moreover, the char yield of the PIs was more than 65% at 800°C in nitrogen. The remarkable thermal stability of the polymers may expand their applications, especially in the area of heat-resistant packing materials.

Color and Optical Properties

The UV–vis spectra of the polymers are shown in Figure 7, and the corresponding data are outlined in Table III. The cutoff wavelengths (λ_{cutoff}'s) were in range 305–365 nm. We measured the transparency of the PIs by averaging the transmittance in the visible region, 400–700 nm. As shown in Table III, the results indicate that the average transmittance of the PI films was in the range 81–90% in the visible region; this was better

Table III. Thermal and Optical Properties of the PIs

Polymer	T_g (°C)[a]	T_d (°C)[b]	$T_{5\%}$ (°C)[c]	$T_{10\%}$ (°C)[c]	Char yield (%)[d]	λ_{cutoff} (nm)	Transparency (%)[e]
PI-1	318	422	445	472	71	324	81
PI-2	294	445	462	484	73	365	86
PI-3	262	441	461	488	74	334	88
PI-4	278	419	440	464	69	323	84
PI-5	277	440	454	471	65	305	90
Kapton[f]	—	—	—	—	—	400	69

[a] Obtained from DSC at a heating rate of 10°C/min in N_2.
[b] T_d obtained from TGA at a heating rate of 10°C/min in N_2.
[c] Recorded by TGA at a heating rate of 10°C/min in N_2.
[d] Char yield (wt %) at 800°C in N_2.
[e] Average transmittance in the visible region (400–700 nm).
[f] According to the literature.[37]

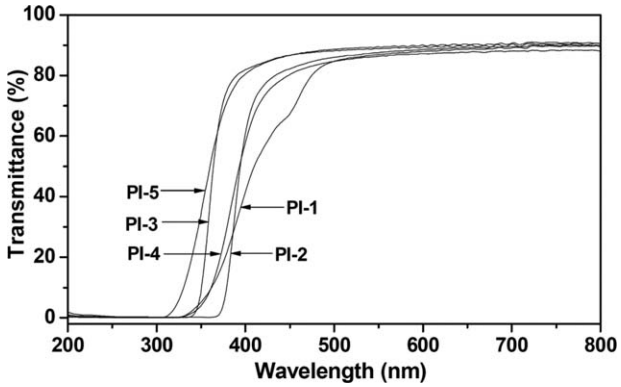

Figure 7. UV–vis spectra of the PI films.

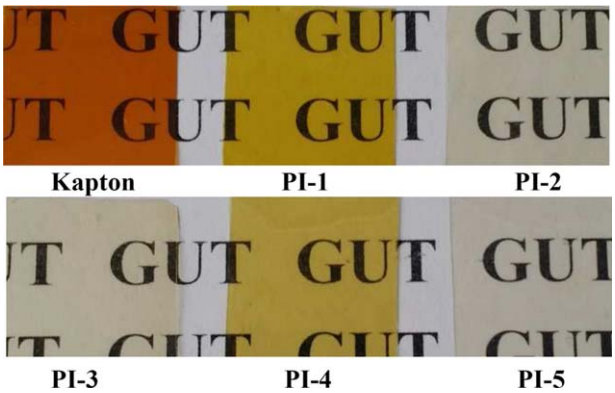

Figure 8. Profile images of the PI films. [Color figure can be viewed in the online issue, which is available at wileyonlinelibrary.com.]

than that of commercial Kapton (69%) according to the literature.[37] Moreover, compared with a Kapton film (Figure 8) with a similar thickness of about 50 μm, the PI films presented a lighter color. Usually, most PIs have a strong absorption in the UV and visible regions, and this is due to the highly conjugated aromatic structures and intermolecular charge-transfer complex (CTC) formation of PIs. However, these PI films exhibited excellent optical properties. This was mainly due to the introduction of bulky isopropyl and biphenyl moieties in the polymer chains, and it reduced the conjugation effect and CTC formation among the aromatic rings of the PI main chains. PI-3 originating from ODPA showed a lighter color and higher average transmittance (88%) because of the incorporation of the flexible ether groups; this weakened the formation of the

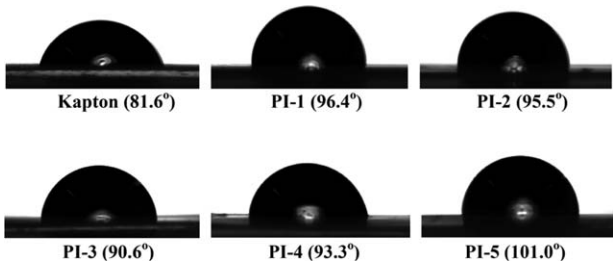

Figure 9. Profiles of water droplets on the Kapton and PI films.

intermolecular CTC effectively. Particularly, PI-5 derived from 6FDA revealed the lowest λ_{cutoff} (305 nm), the lightest color, and the highest average transmittance (90%) because of the introduction of the flexible linkage of fluorinated bulky —$C(CF_3)_2$—; this destroyed the regularity of the polymer backbone and subsequently inhibited the formation of the CTC and decreased the intermolecular cohesive forces because of the lower polarizability of the C—F bond. The high optical transparency and light color of these PI films had potential application prospects in LCDs, optoelectronic devices, light microscopes, and so on.[38]

Mechanical Properties and Dielectric Constants

The mechanical properties of these PI films were measured with a AG-I 50 KN, and the size of film sample was about 50 × 5 × 0.05 mm^3; these data are listed in Table IV. All of the PI films presented excellent tensile strength, elongation at break, and Young's modulus in the ranges 65.6–94.9 MPa, 9.3–13.7%, and 1.6–2.8 GPa, respectively. This indicated that these PI films were strong and tough film materials.

As is known, when polymer materials are used for electronic devices, their dielectric properties are a very important parameter. The dielectric constant of the PI films was tested with a thickness of about 50 μm, as outlined in Table IV. Compared with the dielectric constant of the standard Kapton film (3.48 at 1 MHz), the PI films presented much lower dielectric constant in the range 2.91–3.18 at 1 MHz. The low dielectric constant of the polymers was mainly attributed to the introduction of the bulky substituents, such as isopropyl and biphenyl groups, in the polymer backbone. This decreased the polymer packing density, increased the free volume, and subsequently reduced their dielectric constants. Obviously, PI-5 based on 6FDA exhibited the lowest dielectric constant, and this may have been due

Table IV. Mechanical Properties, Dielectric Constants, and Hydrophobicity Values of the PI Films

Polymer	Tensile strength (MPa)	Elongation at break (%)	Young's modulus (GPa)	Dielectric constant at 1 MHz	θ_w (°)
PI-1	89.5	13.7	1.6	3.10	96.4
PI-2	65.6	12.2	1.7	3.05	95.5
PI-3	94.9	9.3	2.4	2.98	90.6
PI-4	81.3	9.9	2.0	3.18	93.3
PI-5	85.0	10.1	2.8	2.91	101.0
Kapton	—	—	—	3.48	81.6

to the strong electronegativity of fluorine in the polymer chain, which resulted in a lower polarizability of the C—F bonds.[39]

Hydrophobic Properties

PI materials often show relatively higher water absorption values because of the imide group in the main chain.[40] The hydrophobic properties of polymers can be determined by a contact angle tester. Usually, the larger the contact angle is, the stronger the hydrophobic character a polymer has. As shown in Figure 9, the hydrophobic properties of PI films were investigated, and the corresponding data are listed in Table IV. As expected, these polymers exhibited prominent hydrophobic properties, and the contact angles were in the range 90.6–101.0°; these values were higher than that of the standard Kapton film ($\theta_w = 81.6°$). The excellent hydrophobic properties of the polymers were mainly attributed to the introduction of hydrophobic groups, such as isopropyl and biphenyl moieties in the polymer main. The contact angle of PI-1 derived from PMDA was 96.4°, and the polymer presented a relatively good hydrophobicity. This may have been due to the hydrophobic, rigid pyromellitic units in the main chain. Moreover, the PI-5 originating from 6FDA displayed the best hydrophobic properties ($\theta_w = 101.0°$) because of the presence of hydrophobic —CF_3 groups in the polymer chain. This decreased the surface energy of the polymer, and so, it exhibited excellent hydrophobic properties.

CONCLUSIONS

A series of novel PIs containing bulky substituents and noncoplanar structures were prepared from novel aromatic diamine PAPT with various commercial aromatic dianhydrides. All of the PIs presented excellent solubility in common organic solvents, such as DMF, DMAc, DMSO, NMP, $CHCl_3$, CH_2Cl_2, and THF. The PI films also exhibited a high thermal stability, good optical transparency, excellently mechanical properties, and prominent dielectric and hydrophobic properties. The outstanding comprehensive performances of the polymers give them potential applications in the areas of microelectronics, optoelectronics, flexible printed circuit boards, and so on.

ACKNOWLEDGMENTS

This work was financially supported by the National Natural Science Foundation of China (contract grant numbers 51563005, 51163003, and 21264005), the Guangxi Natural Science Foundation (contract grant numbers 2014GXNSFAA118040 and 2013GXNSFDA019008), the Guangxi Ministry–Province Jointly Constructed Cultivation Base for the State Key Laboratory of Processing for Nonferrous Metal and Featured Materials (contract grant number 13KF-3), and the Guangxi Funds for a Specially Appointed Expert.

REFERENCES

1. Ding, M. X. *Prog. Polym. Sci.* **2007**, *32*, 623.
2. Liaw, D. J.; Wang, K. L.; Huang, Y. C.; Lee, K. R.; Lai, J. Y.; Ha, C. S. *Prog. Polym. Sci.* **2012**, *37*, 907.
3. Ghosh, A.; Sen, S. K.; Banerjee, S.; Voit, B. *RSC Adv.* **2012**, *2*, 5900.
4. Liu, C. L.; Chen, W. C. *Polym. Chem.* **2011**, *2*, 2169.
5. Kurosawa, T.; Higashihara, T.; Ueda, M. *Polym. Chem.* **2013**, *4*, 16.
6. Liu, C. J.; Mei, M.; Pei, X. L.; Huang, X. H.; Wei, C. *Chin. J. Polym. Sci.* **2015**, *33*, 1074.
7. Liu, C. J.; Pei, X. L.; Huang, X. H.; Wei, C.; Sun, X. Y. *Chin. J. Chem.* **2015**, *33*, 277.
8. Zhang, S. J.; Bu, Q. Q.; Li, Y. F.; Gong, C. L.; Xu, X. Y.; Li, H. *Mater. Chem. Phys.* **2011**, *128*, 392.
9. Huang, X. H.; Mei, M.; Liu, C. J.; Pei, X. L.; Wei, C. *J. Polym. Res.* **2015**, *22*, 169.
10. Wang, C. Y.; Zhao, X. Y.; Li, G. *Chin. J. Chem.* **2012**, *30*, 2466.
11. Xing, Y.; Wang, D.; Gao, H.; Jiang, Z. H. *J. Appl. Polym. Sci.* **2011**, *122*, 738.
12. Wang, C. Y.; Zhao, H. P.; Li, G.; Jiang, J. M. *Polym. Adv. Technol.* **2010**, *22*, 1816.
13. Chen, J. C.; Wu, J. A.; Chang, H. W.; Lee, C. Y. *Polym. Int.* **2014**, *63*, 352.
14. Li, Y. Q.; Xu, H. H.; Tao, X. A.; Qian, K. J.; Fu, S. A.; Shen, Y. Z.; Ding, S. J. *J. Mater. Chem.* **2011**, *21*, 1810.
15. Zhang, Q. Y.; Li, S. H.; Li, W. M.; Zhang, S. B. *Polymer* **2007**, *48*, 6246.
16. Guan, Y.; Wang, C. B.; Wang, D. M.; Dang, G. D.; Chen, C. H.; Zhou, H. W.; Zhao, X. G. *Polymer* **2015**, *62*, 1.
17. Li, H.; Zhang, S. J.; Gong, C. L.; Liang, Y.; Qi, Z. G.; Li, Y. F. *Polym. Int.* **2015**, *64*, 352.
18. Xia, W. Q.; Xiao, C. H.; Jia, X. L.; Wang, L. *Chem. J. Chin. U.* **2013**, *34*, 2655.
19. Hasegawa, M.; Ishigami, T.; Ishii, J.; Sugiura, K.; Fujii, M. *Eur. Polym. J.* **2013**, *49*, 3657.
20. Dinari, M.; Ahmadizadegan, H. *RSC Adv.* **2015**, *5*, 26040.
21. Hu, B. L.; Wei, H. B.; Han, Y.; Zhu, G. H.; Pei, X. L.; Zhu, J.; Fang, X. Z. *J. Mater. Sci.* **2011**, *46*, 1512.
22. Chang, J. J.; Niu, H. Q.; Zhang, M. Y.; Ge, Q. Y.; Li, Y.; Wu, D. Z. *J. Mater. Sci.* **2015**, *50*, 4104.
23. Lu, Y. H.; Hu, Z. Z.; Wang, Y. F.; Fang, Q. X. *J. Appl. Polym. Sci.* **2012**, *125*, 1371.
24. Huang, X. H.; Huang, W.; Zhou, Y. F.; Yan, D. Y. *Chin. J. Polym. Sci.* **2011**, *29*, 506.
25. Yang, F. C.; Wang, J.; Chen, L.; Wang, X.; Chen, X. Y.; Zhang, X. *Chin. J. Polym. Sci.* **2015**, *33*, 481.
26. Revathi, R.; Prabunathan, R.; Devaraju, S.; Alagar, M. *High Perform. Polym.* **2015**, *27*, 247.
27. Fang, C.; Zhou, Y. M.; He, M.; Bu, X. H.; Yin, K.; Weng, J. J.; Zhang, Z. W. *J. Appl. Polym. Sci.* **2013**, *128*, 80.
28. An, H. Y.; Zhan, M. S.; Wang, K. *J. Appl. Polym. Sci.* **2009**, *114*, 3987.
29. Wiegand, J. R.; Smith, Z. P.; Liu, Q.; Patterson, C. T.; Freeman, B. D.; Guo, R. L. *J. Mater. Chem. A* **2014**, *2*, 13309.
30. Sydlik, S. A.; Chen, Z. H.; Swager, T. M. *Macromolecules* **2011**, *44*, 976.

31. Huang, X. H.; Huang, W.; Liu, J. Y.; Meng, L. L.; Yan, D. Y. *Polym. Int.* **2012**, *61*, 1503.
32. Liaw, D. J.; Wang, K. L.; Chang, F. C.; Lee, K. R.; La, J. Y. *J. Polym. Sci. Part A: Polym. Chem.* **2007**, *45*, 2367.
33. Zhao, X.; Geng, Q. F.; Zhou, T. H.; Gao, X. H.; Liu, G. *Chin. Chem. Lett.* **2013**, *24*, 31.
34. UrRehman, S.; Li, P.; Zhou, H. W.; Zhao, X. G.; Dang, G. D.; Chen, C. H. *Polym. Degrad. Stab.* **2012**, *97*, 1581.
35. Guo, Y. Z.; Shen, D. X.; Ni, H. J.; Liu, J. G.; Yang, S. Y. *Prog. Org. Coat.* **2013**, *76*, 768.
36. Pakhuruddin, M. Z.; Ibrahim, K.; Aziz, A. A. *Optoelectron. Adv. Mater.* **2013**, *7*, 377.
37. Matsumoto, T.; Kurosaki, T. *Macromolecules* **1997**, *30*, 993.
38. Ozser, M. E.; Yucekan, I.; Bodapati, J. B.; Icil, H. *J. Lumin.* **2013**, *143*, 542.
39. Lu, Y. H.; Xiao, G. Y.; Chi, H. J.; Dong, Y.; Hu, Z. Z. *High Perform. Polym.* **2013**, *25*, 894.
40. Hariharan, R.; Sarojadevi, M. *J. Appl. Polym. Sci.* **2006**, *102*, 4127.